Journal of Alloys and Compounds 509 (2011) 805–808

Contents lists available at ScienceDirect

Journal of Alloys and Compounds

journal homepage: www.elsevier.com/locate/jallcom

Effect of Ni substitution on the structural and transport properties of $Ni_xMn_{0.8-x}Mg_{0.2}Fe_2O_4$; $0.0 \leq x \leq 0.40$ ferrite

M.A. Ahmed [a,*], Samiha T. Bishay [b], S.I. El-dek [a], G. Omar [a]

[a] Materials Science Lab (1), Physics Dept., Faculty of Science, Cairo Univ., Giza, Egypt
[b] Phys. Dept., Faculty of Girls for Art, Science and Education, Ain Shams Univ., Cairo, Egypt

ARTICLE INFO

Article history:
Received 8 June 2010
Received in revised form
16 September 2010
Accepted 17 September 2010
Available online 25 September 2010

Keywords:
Ni substituted Mn–Mg ferrite
Dielectric constant
ac conductivity
Correlated barrier hopping

ABSTRACT

$Ni_xMn_{0.8-x}Mg_{0.2}Fe_2O_4$; $0.0 \leq x \leq 0.40$ was prepared by standard ceramic technique, presintering was carried out at 900 °C and final sintering at 1200 °C with heating/cooling rate 4 °C/min. X-ray diffraction analyses assured the formation of the samples in a single phase spinel cubic structure. The calculated crystal size was obtained in the range of 75–130 nm. A slight increase in the theoretical density and decrease in the porosity was obtained with increasing the nickel content. This result was discussed based on the difference in the atomic masses between Ni (58.71) and Mn (54.938). IR spectral analyses show four bands of the spinel ferrite for all the samples. The conductivity and dielectric loss factor give nearly continuous decrease with increasing Ni-content. This was discussed as the result of the significant role of the multivalent cations, such as iron, nickel, manganese, in the conduction mechanism. Anomalous behavior was obtained for the sample with $x = 0.20$ as highest dielectric constant, highest dielectric loss and highest conductivity. This anomalous behavior was explained due to the existence of two divalent cations on B-sites with the same ratio, namely, Mg^{2+} and Ni^{2+}.

1. Introduction

Spinel structure ferrites MFe_2O_4, where M is often a transition metal atom, are a kind of most important magnetic materials and have been widely used in technologies. Manganese ferrites belong to a group of soft ferrite materials characterized by high magnetic permeability and low losses. It is known that the addition of Mg improves the magnetization of Mn ferrite characterized by high saturation magnetization, high electrical resistivity and low loss over a wide range of frequency. These materials are extensively used in many applications such as microwave devices, computer memory chips, magnetic recording media, radio frequency coil fabrication, transformer cores, rod antenna and many branches of telecommunication and electronic engineering.

Several researchers studied the physical properties of ferrites doped by different metals and prepared by different methods [1–4]. $Mg_xMn_{1-x}Fe_2O_4$ ferrite was prepared by the conventional ceramic technique and the hot-pressed ceramic technique [5,6]. Hot pressing of Mg–Mn ferrites results in an improvement of their magnetic and micro-structural properties as it controls simultaneously grain growth and porosity. Substituted Mn ferrites consist of an important category of ceramic magnetic materials with a wide spectrum of technological applications, in devices that in the broadest sense can be characterized as transformers, inductors or absorbers. They are widely used for magnetic applications due to their high permeability and high magnetization. However, their resistivity being low, the eddy current losses at high frequency are very high. Ni ferrites on the other hand possess high resistivity but relatively low permeability at high frequencies. Although substituted Mn and Ni ferrites have been investigated extensively [7–10], literature on the combination of these ferrites is not studied comprehensively and is not quite sufficient. We aimed to merge the advantages of both Ni and Mn ferrites and to profit from the existence of Mg in small constant ratio to assure the large magnetization of the ferrite under investigation. To achieve such goals one have to investigate the effect of Ni substitution on the structural and electrical properties of Mn–Mg ferrite of the chemical formula $Ni_xMn_{0.8-x}Mg_{0.2}Fe_2O_4$; $0 \leq x \leq 0.40$ prepared by conventional ceramic technique.

2. Experimental techniques

High-purity oxides (Aldrich) MnO, NiO, MgO and Fe_2O_3, were mixed thoroughly in stoichiometric ratio, and well grounded in a planetary agate mortar for 3 h. The mixture was pressed into pellets form using uniaxial pressure of 1.9×10^8 N m^{-2} and pre-sintered in air at 900 °C for 10 h with heating rate of 4 °C/min in the Lenton furnace 16/5 UAF (England) then slowly cooled to room temperature with the same rate as that of heating. The samples were grounded again for 1 h and pressed into pellets, then finally sintered in air at 1200 °C for 7 h with the same above conditions. The bulk ceramic samples were finely grounded for check using X-ray diffraction. It was carried out using Philips Pu 1390 channel control Co-kα target and filter Fe of

* Corresponding author. Tel.: +20 2 35676742; fax: +20 2 35676742.
E-mail addresses: moala1947@yahoo.com, moala47@hotmail.com (M.A. Ahmed).

0925-8388/$ – see front matter © 2010 Elsevier B.V. All rights reserved.
doi:10.1016/j.jallcom.2010.09.095

wavelength (λ = 1.791 Å) to assure the formation of the samples with a single spinel phase. The prepared samples were investigated by Fourier Transformation Infrared FTIR spectrometer model 300E, in the range of 200–1000 cm^{-1}. A pellet of about 0.85 cm diameter and 0.2 cm thick were used to measure the electrical properties. The two surfaces of each sample were finely polished, coated with silver paste and checked for good conduction. The ac resistivity as well as the dielectric constant of the investigated samples was measured from room temperature up to 700 °C as a function of frequency ranging from 100 kHz to 5 MHz using RLC Bridge (HIOKI model 3531 Z Hi Tester "Japan"). The measurements were carried out using a home built Lab-View program that is suitable for dielectric measurements. The measurement accuracy was better than 1%.

3. Results and discussion

Fig. 1 shows the X-ray diffraction patterns for $Ni_xMn_{0.8-x}Mg_{0.2}Fe_2O_4$ $(0 \le x \le 0.40)$. All the diffractograms confirmed the formation of the single phase ferrite with cubic spinel structure as compared with ICDD card number 2-1034. From the data one can find that, for all concentrations all planes characterizing the single spinel ferrite phase exist and the peak intensity depends on the concentration of magnetic ions in the lattice. The lattice parameter of the investigated cubic spinel system (where $a = b = c$) was calculated using the formula [8]:

$$a = d_{hkl}\sqrt{(h^2 + k^2 + l^2)} \quad (1)$$

The data in Fig. 2a clarify that the lattice parameter decreases with increasing Ni content, this can be attributed to the replacement of larger Mn^{2+} (0.83 Å) by smaller ions Ni^{2+} ions (0.69 Å) [9]. The average crystal size (L) was calculated from the experimental data using Debye–Scherrer formula [8] and clarified in Fig. 2b. It is noted that there is a slight decrease in L with Ni content except for the sample $x = 0.20$. At this concentration Ni^{2+} and Mg^{2+} ions are expected to be equi-distributed on the B sites. The variation of the crystal size with Ni content is mainly due to the resultant microstrain produced from the difference between the ionic radii of Ni^{2+} and Mn^{2+} ions. The variation of X-ray density D_x with Ni content is illustrated in Fig. 2c. The data show that D_x increases with increasing Ni content which is due to the difference in the atomic masses between Ni (58.71) and Mn (54.938) as well as the remarkable decrease in the lattice volume. The percentage porosity (P) was calculated using the relation [10]:

$$P = 1 - \frac{D}{D_x} \quad (2)$$

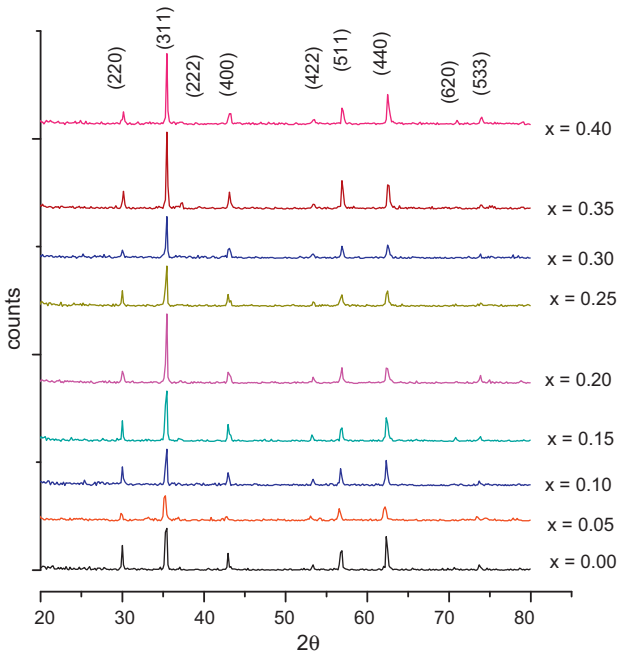

Fig. 1. X-ray diffractograms of $NixMn_{0.8-x}Mg_{0.2}Fe_2O_4$ $(0 \le x \le 0.40)$ prepared by standard ceramic technique sintered at 1200 °C with a heating rate 4 °C/min.

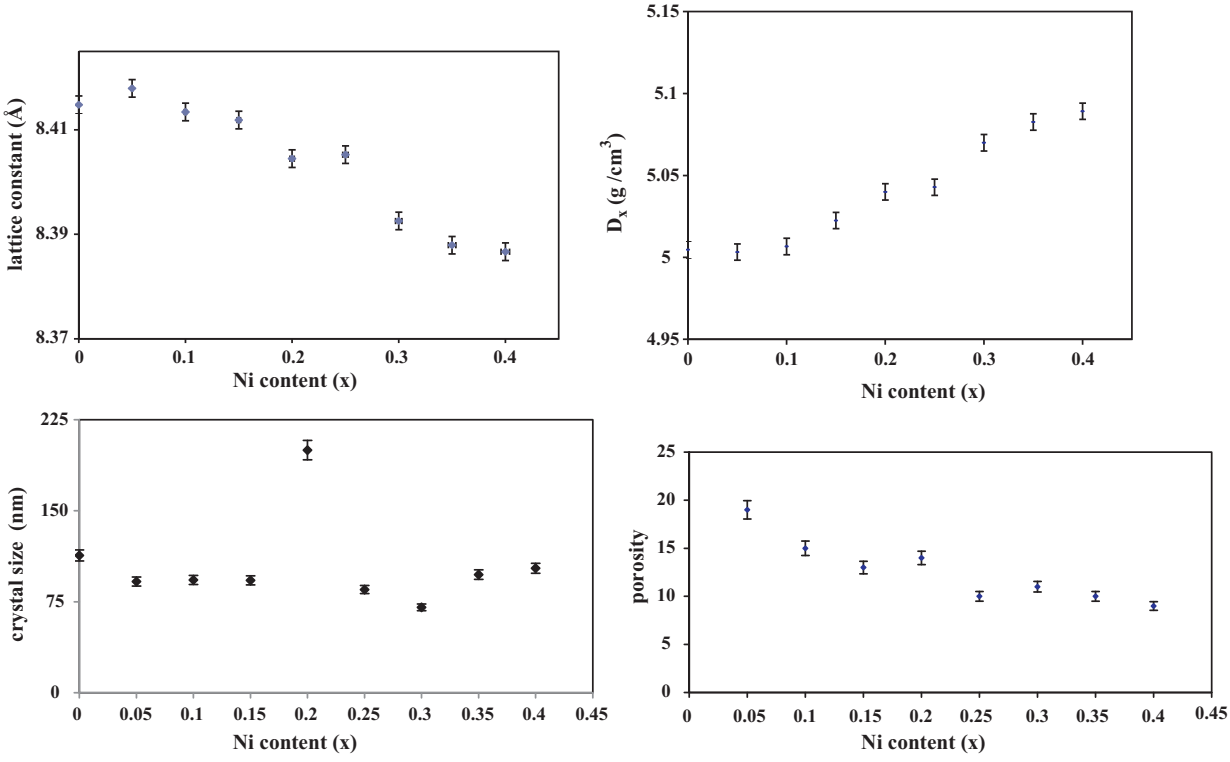

Fig. 2. (a) The dependence of lattice parameter on Ni content for $Ni_xMn_{0.8-x}Mg_{0.2}Fe_2O_4$; $0 \le x \le 0.40$. (b) The dependence of the crystal size on Ni content for the samples $Ni_xMn_{0.8-x}Mg_{0.2}Fe_2O_4$; $0 \le x \le 0.40$. (c) The dependence of X-ray density on Ni content for the samples $Ni_xMn_{0.8-x}Mg_{0.2}Fe_2O_4$; $0 \le x \le 0.40$. (d) The dependence of the porosity on the Ni content for the samples $Ni_xMn_{0.8-x}Mg_{0.2}Fe_2O_4$; $0 \le x \le 0.40$.

where D is the experimental density. The variation of the porosity as a function of Ni content is illustrated in Fig. 2d. From the data in the figure it is shown that, the porosity decreases with increasing Ni content, which is attributed to the substitution of Ni^{2+} of large ionic radius (0.69 Å) by Fe^{3+} of ionic radius (0.645 Å) [5].

IR spectra are shown in Fig. 3 for samples $Ni_xMn_{0.8-x}Mg_{0.2}Fe_2O_4$ ($0 \le x \le 0.40$) recorded in the range of 200–800 cm^{-1}. As usual for spinel ferrites, the band υ_1 from 633 to 692 cm^{-1} arises due to the tetrahedral metal–oxygen bond $(Fe^{3+}–O^{2-})_{tetra}$ and υ_2 from 582 to 584 cm^{-1} is due to the octahedral metal–oxygen $(Fe^{3+}–O^{2-})_{octa}$ and these two bands are characteristic for Ni–Mn ferrite as reported elsewhere [11–14]. Also, it has been reported that [15], $Fe^{3+}–O^{2-}$ distance for A-site (0.189 nm) is smaller than that of B-site (0.199 nm). This was interpreted by more covalent bonding of Fe^{3+} ions at the A-site. Fig. 3 illustrates the appearance of the other two spinel characteristic bands υ_3 and υ_4 around 370 and 200 cm^{-1} respectively. These two bands are assigned to $M^{2+}–O^{2-}$ complexes vibration on B-site and lattice vibration respectively. A closer look to Fig. 3 shows that the bands υ_1, υ_2, and υ_3 for $Ni_xMn_{0.8-x}Mg_{0.2}Fe_2O_4$ ($0 \le x \le 0.40$) are shifted to higher frequencies and at $x = 0.10$ there is no thought for the second band and this may be due to overlapping between bands.

The variations in dielectric constant of ferrite have been mainly attributed to the variation in concentration of Fe^{2+} [16–18]. The greater the concentration of this ion, the higher the dielectric constant expected. The presence of Fe^{2+} ions results in charge transfer of the type $Fe^{2+} \leftrightarrow Fe^{3+} + e^-$ causing a local displacement of electron in the direction of electric field leading to polarization. Multivalent cations, such as Fe, Ni, Mn, play the key role in the conduction process for this kind of ferrite [19]. In general, the polarizability and conductivity have the same origin in ferrites [20,21], which is due to electron exchange between Fe^{2+} and Fe^{3+} ions on octahedral sites.

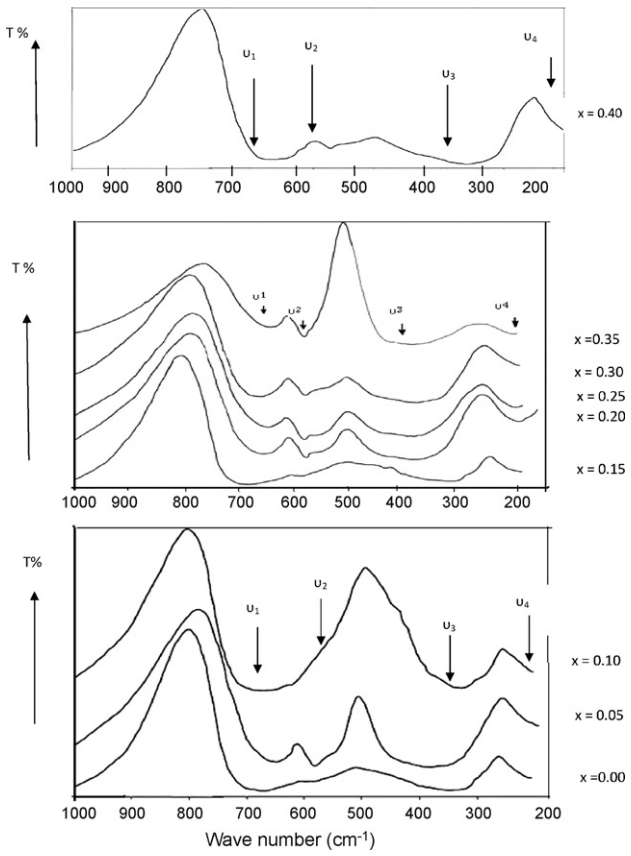

Fig. 3. IR transmission spectra of $Ni_xMn_{0.8-x}Mg_{0.2}Fe_2O_4$ ($0 \le x \le 0.40$).

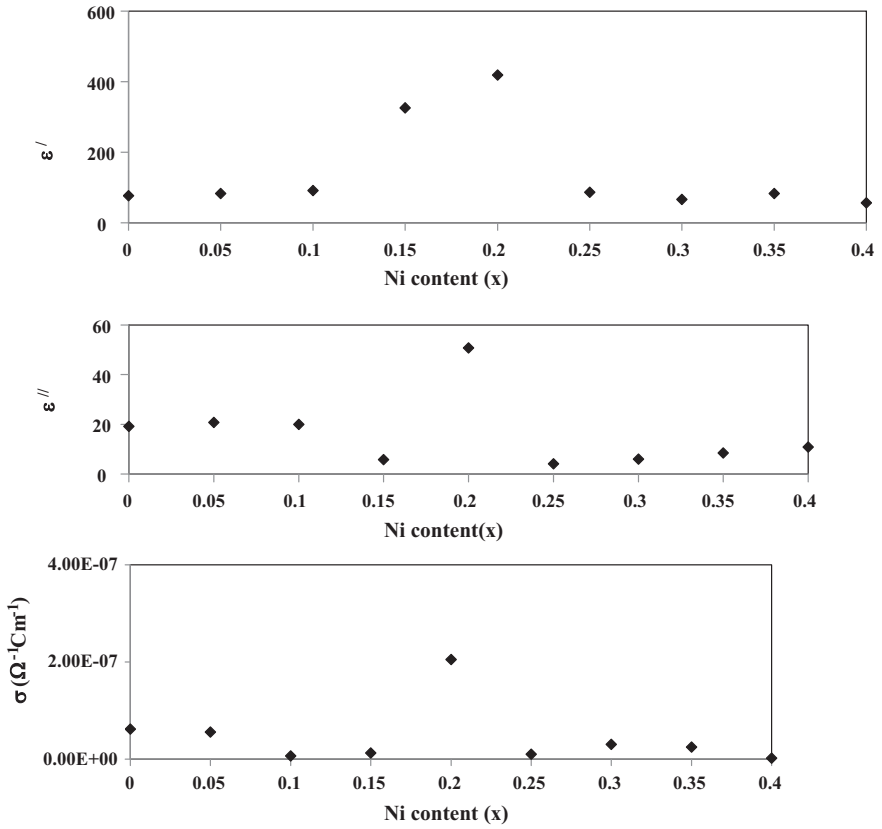

Fig. 4. (a–c) The dependence of the dielectric constant, the dielectric loss factor and the conductivity on Ni content for $Ni_xMn_{0.8-x}Mg_{0.2}Fe_2O_4$ ($0 \le x \le 0.40$) at 100 kHz and 350 K.

Table 1
The calculated exponent factor (s) for $Ni_xMn_{0.8-x}Mg_{0.2}Fe_2O_4$; $0.0 \le x \le 0.40$ at selected temperatures.

T (K)	$x=0$	$x=0.05$	$x=0.10$	$x=0.15$	$x=0.20$	$x=0.25$	$x=0.30$	$x=0.35$	$x=0.40$
400	0.73	0.33	0.71	0.90	0.79	0.86	0.56	0.90	0.88
600	0.66	0.24	0.12	0.25	0.46	0.16	0.11	0.13	0.23
700	0.12	0.16	0.12	0.23	0.24	0.12	0.05	0.04	0.09

Fig. 4a–c correlates the dependence of ε', ε'' and σ on the Ni content for $Ni_xMn_{0.8-x}Mg_{0.2}Fe_2O_4$ ($0 \le x \le 0.40$) at 350 K at 100 kHz. From the figure, it is noticed that, the dielectric constant increases with increasing Ni content up to $x = 0.20$ and then decreases afterward. While for the conductivity and dielectric loss factor, it nearly continues to decrease with increasing x with anomaly at the sample with $x = 0.20$. Generally, doping with Ni^{2+} ions decreases the hopping between Fe^{3+} and Fe^{2+} ions, thereby increasing the resistance of the grains which leads to a slight decrease in the conductivity. The probability of reaching the electron boundary is thus reduced. As a result, the polarization and hence, the dielectric constant decrease. The concentration of $x = 0.20$ is considered as a critical Ni^{2+} content at which maximum electron hopping occurred. This is due to the contribution of more than one valance exchange at this content. After $x = 0.20$, one can expect that the electrons resulting from (Fe^{2+}, Fe^{3+}) and (Mn^{2+}, Mn^{3+}) are captured by Ni^{3+} ions to be retransformed into Ni^{2+} ions. This in turns is reflected in the conductivity as it has the same origin of polarization. Maximum loss is observed also at $x = 0.20$ which agrees well with the maximum conductivity, at which the cluster formation can occur and acts as trapping center at different depths. Moreover, Ni content of $x = 0.20$ exhibits maximum crystal size. The correlation here could be due to the change in anisotropy of the ferrite. Moreover, at $x = 0.20$ two divalent cations exist on B-sites with the same ratio, namely, Mg^{2+} and Ni^{2+}.

The magnitude of the gradient (change in the conductivity with respect to temperature) depends on the exchange interaction between the outer and inner electron of the metal ions, which is changed at the transition temperature (Curie temperature) transferring the system from the ordered to disordered state [22]. The calculated activation energy E_I and E_{II}, from the conductivity data for $Ni_xMn_{0.8-x}Mg_{0.2}Fe_2O_4$; $0.0 \le x \le 0.40$ is shown in Fig. 5. It is clear that the activation energy in the paramagnetic region (disorder state) (E_{II}) is greater than that in the ferromagnetic (E_I) region [23]. This is due to the effect of spin order [24] and the effect of large energy needed to liberate the electrons and activate them to participate in conduction process [21].

The ac conductivity is governed by the relation [25–27]:

$$\sigma_{ac} = A\omega^s \quad (3)$$

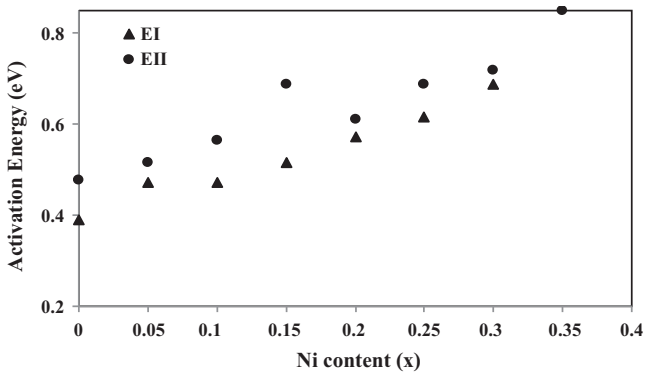

Fig. 5. The dependence of the activation energies E_I and E_{II} on Ni content at 100 kHz for the samples $Ni_xMn_{0.8-x}Mg_{0.2}Fe_2O_4$, where $0 \le x \le 0.40$.

The exponent values (s) are calculated as the slope of the straight lines obtained from the relation between $\ln(\sigma_{ac})$ and $\ln(\omega)$ and reported in Table 1. It is noted that for all samples s decreases with increasing temperature obeying the Correlated Barrier Hopping (CBH) model. In our case the conductivity is mainly due to the following electron hopping simultaneously between (Ni^{2+}, Ni^{3+}), (Mn^{2+}, Mn^{3+}) and (Fe^{2+}, Fe^{3+}) on the B-sites. The increase in the conductivity is due to thermal activation of charge carriers, i.e. the increase of charge carriers drift mobility and not their number.

4. Conclusion

The investigated ferrite samples $Ni_xMn_{0.8-x}Mg_{0.2}Fe_2O_4$; $0.0 \le x \le 0.40$ prepared by standard ceramic technique with crystal size ranged from 75 nm to 130 nm characterized by:

1. A slightly increase in the theoretical density and decrease in the porosity was obtained with increasing the nickel content.
2. The conduction mechanism for all these samples is correlated barrier hopping mechanism.
3. The conductivity and dielectric loss factor decrease with increasing the Ni-content.
4. Anomalous dielectric behavior was obtained for the sample with $x = 0.20$ as highest dielectric constant, highest dielectric loss and highest conductivity.

References

[1] M.A. Ahmed, S.T. Bishay, Mater. Chem. Phys. 114 (2009) 446–450.
[2] M.A. Ahmed, N. Okasha, S.I. El-Dek, Nanotechnology 19 (2008) 065603.
[3] M.A. Ahmed, S.F. Mansour, S.I. El-dek, Physica B 403 (2008) 224–230.
[4] M.A. Ahmed, S.T. Bishay, J. Phys. D: Appl. Phys. 34 (2001) 1339–1345.
[5] M. Singh, J. Magn. Magn. Mater. 299 (2006) 397–403.
[6] M. Ajmal, A. Maqsood, Mater. Lett. 62 (2008) 2077.
[7] Z.G. Zheng, X.C. Zhong, Y.H. Zhang, H.Y. Yu, D.C. Zeng, J. Alloys Compd. 466 (2008) 377.
[8] A.A. Sattar, H.M. El-Sayed, K.M. El-Shokrofy, M.M. El-Tabey, J. Mater. Eng. Perform. 14 (2005) 99.
[9] R.D. Shannon, Acta Crystallogr. A 32 (1976) 751–767.
[10] M.U. Islam, I. Ahmed, T. Abaas, Proceeding of Sixth International Symposium on Advanced Material, 1999.
[11] O.M. Hemeda, J. Magn. Magn. Mater. 281 (2004) 36–41.
[12] M.K. Shobana, S. Sankar, V. Rajendran, J. Alloys Compd. 472 (2009) 421–424.
[13] M.R. Anantharaman, S. Jagatheesan, S. Sindhu, K.A. Maini, A. Narayanasamy, C.N. Chinnasamy, K. Philip, K. Vasudevan, Int. J. Plast. Rubber Process. Appl. 27 (1998) 77–81.
[14] M.A. Amer, Phys. Status Solidi A 151 (1995) 205.
[15] M.Z. Said, Mater. Lett. 34 (1998) 305–307.
[16] N. Rezlescu, E. Rezlescu, Phys. Status Solidi A 23 (1974) 575.
[17] J.T.S. Irvine, A. Huanosta, R. Velenzula, A.R. West, J. Am. Ceram. Soc. 88 (1990) 729.
[18] C.G. Koops, Phys. Rev. 83 (1951) 121.
[19] P.R. Mahasjan, K.K. Patankar, M.B. kothale, S.C. Chaudhari, V.L. Math, S.A. Patil, Pramana 58 (2002) 2341.
[20] L. Neel, Ann. Phys. 3 (1948) 137–198.
[21] E Ateia, M.A. Ahmed, A.K. El-Aziz, J. Magn. Magn. Mater. 311 (2007) 545–554.
[22] M.A. Ahmed, E. Ateia, L.M. Salah, A.A. El-Gamal, Mater. Chem. Phys. 92 (2005) 310–321.
[23] Y.P. Irkhin, E.A. Turov, Sovt. Phys. JEPT 33 (1975) 673.
[24] D.J. Carrick, Magentic Oxides Part-I, Wiley Interscience, London, 1975.
[25] G.E. Pike, Phys. Rev. B 6 (1972) 1572.
[26] S.R. Eliot, E.A. Davis, 7th Int. Conf. on Amorphous and Liquid Semiconductors, Edinburgh, 1977, p. 637.
[27] S.S. Ata-Allah, M. Kasir, J. Alloys Compd. 471 (2009) 303–309.